Gazi Üniversitesi
Fen Bilimleri Dergisi
PART C: TASARIM VE TEKNOLOJİ

Gazi University
Journal of Science
PART C: DESIGN AND TECHNOLOGY

GU J Sci, Part C, 14(1): 305-317 (2026)

Geotechnical Investigation of a Construction-Site Failure: Insights from Field and Numerical Analyses

Temel KÖROĞLU[1*], Pınar Sezin ÖZTÜRK KARDOĞAN[2*], Ahmet ERDAĞ[3*], Latif YEŞİL[4]

[1]*MSc Student, Gazi University, Graduate School of Natural and Applied Sciences*

[2]*Asist. Prof. Dr., Gazi University, Faculty of Technology, Department of Civil Engineering*

[3]*Dr., Kafkas University, Faculty of Engineering and Architecture, Department of Civil Engineering*

[4]*Eng., Ankara Metropolitan Municipality, Department of Survey and Project Development*

Article Info

Research article
Received: 25/112025
Revision:13/12/2025
Accepted: 25/12/2025

Keywords

Slope stability, Groundwater effects, Finite element analysis, Geotechnical investigation

Makale Bilgisi

Araştırma makalesi
Başvuru: 25/112025
Düzeltme: 13/12/2025
Kabul: 25/12/2025

Anahtar Kelimeler

Şev stabilitesi, Yeraltı suyunun etkileri, Sonlu elemanlar analizi, Geoteknik araştırma

Graphical/Tabular Abstract (Grafik Özet)

This study investigates excavation-induced slope instability through integrated field investigations and numerical analyses, emphasizing groundwater effects and support system performance under static and pseudo-static conditions. / Bu çalışma, kazı kaynaklı şev dengesizliğini arazi verileri ve sayısal analizlerin kullanımıyla inceleyerek su seviyesi etkilerini ve destek sistemlerinin davranışını ortaya koymaktadır.

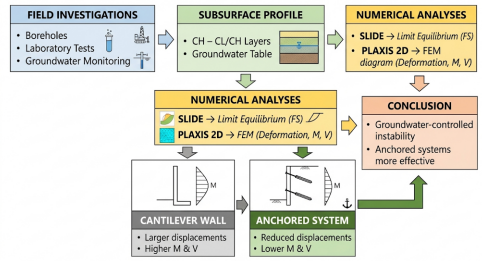

***Figure A**: Stability Analysis and Retaining System Optimization for Deep Excavations. / **Şekil A:** Derin kazılar için stabilite analizi ve iksa sistemi optimizasyonu*

Highlights (Önemli noktalar)

- *Groundwater conditions play a dominant role in long-term slope instability. / Yeraltı suyu koşulları uzun dönem şev dengesizliğinde belirleyici rol oynamaktadır.*
- *Limit equilibrium and finite element methods provide complementary insights into failure mechanisms. / Limit denge ve sonlu elemanlar yöntemleri göçme mekanizmalarını tamamlayıcı biçimde ortaya koymaktadır.*
- *Anchored retaining systems significantly reduce lateral displacements and internal forces. / Ankrajlı iksa sistemleri yatay deplasmanları ve iç kuvvetleri önemli ölçüde azaltmaktadır.*

***Aim (Amaç):** To evaluate excavation-induced slope instability by integrating subsurface investigations with limit equilibrium and finite element analyses under static, pseudo-static, and seepage conditions. / Kazı kaynaklı şev dengesizliğini statik, yarı-statik ve sızıntı koşulları altında zemin araştırmaları ile sayısal analizleri bütünleştirerek değerlendirmektir.*

***Originality (Özgünlük):** The study uniquely combines detailed groundwater assessment with comparative numerical evaluation of anchored and cantilever retaining systems for deep excavations in clayey alluvial soils. / Bu çalışma, kil ağırlıklı alüvyon zeminlerde derin kazılar için yeraltı suyu etkileriyle birlikte ankrajlı ve konsol iksa sistemlerini karşılaştırmalı olarak ele alması açısından özgündür.*

***Results (Bulgular):** Analyses indicate that long-term drained conditions reduce safety factors below unity at 5.0 m and 6.5 m excavation depths, while anchored systems effectively limit lateral displacements to approximately 1.5–1.6 cm. / Analizler, uzun dönem drenajlı koşullarda 5.0 m ve 6.5 m kazı derinliklerinde güvenlik katsayısının 1.0'ın altına düştüğünü; ankrajlı sistemlerin ise yatay deplasmanları yaklaşık 1.5–1.6 cm ile sınırladığını göstermektedir.*

***Conclusion (Sonuç):** The study demonstrates that reliable slope stability assessment in excavation projects requires hydro-mechanically coupled analyses and advanced numerical modeling, with anchored retaining systems providing superior performance under complex geotechnical conditions. / Bu çalışma, kazı projelerinde güvenilir şev stabilitesi değerlendirmesi için hidro-mekanik etkileşimleri içeren gelişmiş sayısal analizlerin gerekliliğini ortaya koymakta; ankrajlı iksa sistemlerinin karmaşık jeoteknik koşullarda daha etkin çözümler sunduğunu göstermektedir.*

*Corresponding author, e-mail: sezinozturk@gazi.edu.tr
DOI: 10.29109/gujsc.1830035

GU J Sci, Part C, 14(1): 305-317 (2026)

Gazi Üniversitesi
Fen Bilimleri Dergisi
PART C: TASARIM VE TEKNOLOJİ

Gazi University
Journal of Science
PART C: DESIGN AND TECHNOLOGY

http://dergipark.gov.tr/gujsc

Geotechnical Investigation of a Construction-Site Failure: Insights from Field and Numerical Analyses

Temel KÖROĞLU[1*], Pınar Sezin ÖZTÜRK KARDOĞAN[2*], Ahmet ERDAĞ[3*], Latif YEŞİL[4]

[1]*MSc Student, Graduate School of Natural and Applied Sciences*

[2]*Asist. Prof. Dr., Gazi University, Faculty of Technology, Department of Civil Engineering*

[3]*Dr., Kafkas University, Faculty of Engineering and Architecture, Department of Civil Engineering*

[4]*Eng., Ankara Metropolitan Municipality, Department of Survey and Project Development*

Article Info

Research article
Received: 25/112025
Revision:13/12/2025
Accepted: 25/12/2025

Keywords

Slope stability,
Groundwater effects,
Finite element analysis,
Geotechnical investigation

Abstract

This study presents a comprehensive evaluation of the causes of slope instability observed at a construction site characterized by complex geotechnical conditions. It is well recognized that slope stability problems rarely result from a single factor; rather, they arise from the combined effects of multiple parameters, including soil lithology and plasticity characteristics, discontinuities, groundwater level, rainfall–infiltration processes, dynamic loading conditions, and excavation geometry. In this context, the subsurface profile of the study area was defined in detail through borehole investigations, laboratory testing, and groundwater observations. Subsequently, slope behavior was analyzed under static, pseudo-static, and seepage-induced conditions. Critical slip surfaces and factors of safety were determined using the limit equilibrium–based SLIDE software, while the behavior, deformations, and internal force distributions of excavation support systems were evaluated using the finite element–based PLAXIS 2D program. The results indicate that groundwater level and drainage conditions significantly increase pore water pressures along critical slip surfaces, thereby triggering instability. Consistent with the literature, even minor variations in geotechnical parameters were found to cause pronounced changes in the factor of safety, while inadequate drainage conditions accelerated stability loss. Overall, the study systematically addresses the multifactorial nature of slope instability from an engineering perspective and provides an integrated assessment that combines field data with advanced numerical modeling. The findings contribute to the development of safe, optimized, and technically robust slope design solutions under complex geotechnical conditions.

Bir İnşaat Sahasındaki Zemin Probleminin Geoteknik İncelemesi: Arazi ve Sayısal Analizlerden Elde Edilen Bulgular

Makale Bilgisi

Araştırma makalesi
Başvuru: 25/112025
Düzeltme: 13/12/2025
Kabul: 25/12/2025

Anahtar Kelimeler

Şev stabilitesi,
Yeraltı suyunun etkileri,
Sonlu elemanlar analizi,
Geoteknik araştırma

Öz

Bu çalışma, karmaşık jeoteknik koşullara sahip bir şantiye alanında meydana gelen şev dengesizliğinin nedenlerini kapsamlı biçimde değerlendirmektedir. Şev stabilitesi problemlerinin genellikle tek bir etkene bağlı olmadığı; zemin litolojisi ve plastisite özellikleri, süreksizlikler, yeraltı suyu seviyesi, yağış–infiltrasyon süreçleri, dinamik yükler ve kazı geometrisi gibi çok sayıda parametrenin etkileşimi sonucu ortaya çıktığı vurgulanmaktadır. Bu kapsamda, çalışma alanının yeraltı profili sondaj çalışmaları, laboratuvar deneyleri ve yeraltı suyu gözlemleriyle ayrıntılı olarak tanımlanmıştır. Şev davranışı statik, yarı-statik ve sızıntı etkili koşullar altında analiz edilmiş; kritik kayma yüzeyleri ve güvenlik katsayıları limit denge esaslı SLIDE yazılımı ile belirlenmiştir. Kazı destek sistemlerinin deformasyonları ve iç kuvvet dağılımları ise sonlu elemanlar tabanlı PLAXIS 2D programı kullanılarak değerlendirilmiştir. Analiz sonuçları, yeraltı suyu seviyesi ve drenaj koşullarının boşluk suyu basınçlarını artırarak dengesizliği tetiklediğini ortaya koymaktadır. Ayrıca, zemin parametrelerindeki küçük değişimlerin güvenlik katsayısı üzerinde belirgin etkiler yarattığı ve yetersiz drenajın stabilite kaybını hızlandırdığı gözlenmiştir. Sayısal analizler, 5.0 m ve 6.5 m kazı derinliklerinde uzun dönem drenajlı koşullarda güvenlik katsayısının 1.0'ın altına düştüğünü; ankrajlı iksa sistemlerinin ise yatay deplasmanları sınırlayarak konsol sistemlere kıyasla daha güvenli ve etkin bir çözüm sunduğunu göstermektedir.

*Corresponding author, e-mail: sezinozturk@gazi.edu.tr
DOI: 10.29109/gujsc.1830035

1. INTRODUCTION (GİRİŞ)

Slope stability represents one of the most complex and multidisciplinary domains of geotechnical engineering, as the accurate modelling of potential instabilities in natural or man-made slopes requires the simultaneous evaluation of soil mechanics, rock mechanics, hydrogeology, engineering geology, and advanced numerical analysis techniques. Slope failures typically evolve as a consequence of multiple weakening mechanisms acting concurrently, rather than a single triggering factor. Instability is commonly initiated when critical threshold values of various parameters—such as soil lithology, grain-size distribution, plasticity characteristics, discontinuities, groundwater level, rainfall–infiltration processes, seismic accelerations, external loadings, and excavation geometry—are exceeded. Engineering activities on construction sites, particularly stress relief following deep excavations and sudden changes in slope geometry, can further aggravate instability. This condition was prominently demonstrated in a previous investigation, which indicated that excavation-induced slope problems are strongly dependent on soil properties and excavation sequence, and that instability potential increases rapidly when groundwater conditions are incorporated into the assessment [1].

Traditional limit equilibrium methods, although widely used in engineering practice to estimate safety factors for circular or composite slip surfaces, are insufficient to fully capture deformation mechanisms, stress redistribution, and time-dependent hydro-mechanical interactions of soil masses. Consequently, contemporary engineering studies increasingly rely on finite element methods employing elasto-plastic soil models such as Mohr–Coulomb, Hardening Soil, and Drucker–Prager, as well as shear strength reduction techniques, which enable a more realistic determination of the position of critical slip surfaces, zones of plasticization, pore-water pressure development, and overall stability behavior [2].

One of the most fundamental parameters governing slope behavior is the suite of engineering properties of soils. Variables such as cohesion (c), internal friction angle (φ), unit weight (γ), void ratio (e), and hydraulic conductivity (k) have a decisive influence on shear strength, as extensively demonstrated in the literature. Previous studies reported that increases in cohesion and friction angle significantly improve safety factors, while geosynthetic reinforcement considerably enhances stability in weak soils [3,4]. Other research emphasized that slope response under dynamic loading conditions strongly interacts with soil class, topography, and spectral acceleration characteristics [5].

Hydrogeological conditions constitute another critical factor influencing slope stability. Rainfall, infiltration, rising groundwater levels, and insufficient drainage increase pore-water pressures within the soil mass, decrease effective stresses, and push critical slip surfaces toward failure conditions. Recent studies have therefore underlined the necessity of incorporating seepage mechanisms into stability assessments. It has been shown that increasing horizontal drainage length improves safety factors up to a threshold value, beyond which additional drainage does not yield significant improvement. A reduction in pore-water pressures following the lowering of the water table clearly highlights the direct relationship between stability and the prevailing seepage regime [6,7].

Other significant processes affecting slope stability have also been detailed in the literature. Dynamic stresses generated by blasting operations may weaken discontinuities and adversely influence long-term stability, while rising groundwater levels and low drainage capacity can lead to rapid losses in stability [8,9]. Furthermore, back-analysis studies highlight that identifying accurate soil parameters and employing multiple analysis approaches simultaneously are essential for reliable evaluations [10].

Research on geomaterials has also provided valuable insights into how material composition, environmental conditions, and loading characteristics influence soil behavior. Investigations involving plastic waste and construction by-products have shown that alternative materials can modify soil stiffness and drainage behavior under varying boundary conditions [11,12]. Additional studies focusing on reinforced and unreinforced geomaterials subjected to repeated loading have emphasized the sensitivity of deformation mechanisms to stress levels, pore-water pressures, and material structure [13,14]. Such findings underline the broader importance of understanding material–environment interactions, which are also central to evaluating slope stability under complex geotechnical conditions.

Building upon this extensive body of knowledge, the present study aims to comprehensively investigate the geotechnical and structural causes of slope instability observed at a construction site. Through borehole investigations, laboratory tests,

groundwater observations, and soil classification studies, the subsurface profile has been thoroughly characterized. The static, pseudo-static, and seepage-induced hydro-mechanical behavior of the slope has been analyzed using advanced numerical modelling techniques. Critical slip surfaces, potential failure mechanisms, and corresponding safety factors have been identified, and the root causes of instability along with appropriate engineering mitigation measures have been systematically examined.

In this regard, the study provides a comprehensive engineering assessment that integrates site-specific soil data, hydrogeological conditions, and advanced numerical modelling approaches. The findings aim to contribute to the development of safe, sustainable, and optimized slope designs under complex geotechnical conditions.

2.SITE DESCRIPTION AND GEOTECHNICAL CONDITIONS (SAHA ÖZELLİKLERİ vVE GEOTEKNİK KOŞULLAR)

2.1. Geomorphological and Environmental Characteristics (Jeomorfolojik ve Çevresel Özellikler)

The study area is located within parcel no. 46937, block 3, Bağlıca District, Etimesgut, Ankara, where the construction of a sports complex project is planned. Ankara is situated in the central part of the Central Anatolia Region and bordered by Kırıkkale to the east, Çankırı to the northeast, Bolu to the northwest, Eskişehir to the west, Konya to the south, and Kırşehir and Aksaray to the southeast.

The regional topography generally exhibits a gently undulating plain morphology, with surface drainage primarily governed by the Sakarya River and its tributaries.

The geomorphological setting of Ankara consists of extensive alluvial plains, local uplands, and tectonically induced depression basins. A distinct elevation difference exists within the project area: the highest building corner elevation is 934.50 m, while the lowest is 932.90 m. The reference elevation (±0.00) is defined as 933.36 m, and the average foundation level is approximately 927.96 m, indicating excavation depths ranging between 4.9 and 6.5 m. The structure is designed with a raft foundation system and planned as one basement, one ground, and one upper floor.

2.2. Regional Geology (Bölgesel Jeoloji)

The lithostratigraphic succession observed in Etimesgut and its vicinity, from oldest to youngest, comprises the Akbayır, Hançili, and Gölbaşı Formations, overlain unconformably by Quaternary alluvial deposits [15].

•Akbayır Formation (Ja): Consists of thin- to medium-bedded cherty and biomicritic limestones. The lower levels are composed of interbedded marl, siltstone, and clayey limestone, transitioning upward into hemipelagic limestone layers.

•Hançili Formation (Th): Characterized by alternating marl, claystone, siltstone, sandstone, conglomerate, and tuffite layers. Locally includes gypsum and bituminous shale interbeds. The formation is dated to the Serravallian–Tortonian age.

•Gölbaşı Formation (Tg): Composed of poorly cemented gray, reddish, and brownish conglomerates, sandstones, and siltstones. The formation is of Upper Miocene–Pliocene age.

•Alluvium (Qa): Representing the youngest unit in the study area, these Quaternary deposits consist of gravel, sand, silt, and clay with loose, uncemented structures. They exhibit low cohesion and high permeability, which are critical factors affecting slope stability.

2.3. Seismicity (Sismik Aktivite)

According to the Turkish Seismic Hazard Map (AFAD, 2018), Ankara lies within a DD-2 seismic hazard zone [16]. Although the city itself is not situated directly on an active fault, two major fault systems influence its seismic response: The North Anatolian Fault Zone (NAFZ) located approximately 100 km to the north, and the Kırşehir–Keskin Fault Zone located about 90–100 km to the southeast.

While the probability of a major earthquake in the region is relatively low, ground motions generated by moderate ($M < 5.5$) earthquakes from nearby fault systems may still affect local ground stability. Consequently, such dynamic influences were considered significant for the static stability assessment of the planned excavation.

According to AFAD's Earthquake Hazard Maps of Turkey Interactive Web Application, the design parameters required for pseudostatic analysis in medium-dense to dense sands, gravels, or stiff clay layers (DD-2 seismic hazard level, corresponding to

a 10% probability of exceedance in 50 years, i.e., a 475-year return period) are as follows: S_S = 0.319, F_S =1.545. The design spectral acceleration coefficient is computed as $S_{DS} = (S_S)x(F_S) = 0.319 \times 1.545 = 0.493$

$$k_h = 0.2\ S_{DS} \ ; \quad k_v = 0.5\ k_h$$

$k_h = 0.2x0.493=0.0986$; $k_v=0.5x0.0986=0.0493$

In accordance with TBDY (2018), the horizontal and vertical static-equivalent earthquake coefficients used in slope stability analyses are defined as $k_h = 0.2\ S_{DS}$ and $k_v = 0.5\ k_h$. Using these expressions, the horizontal coefficient was obtained as k_h = 0.0986, and the corresponding vertical coefficient as k_v = 0.0493.

2.4. Subsurface Investigation and Soil Profile
(Zemin Altı Araştırmaları ve Zemin Profili)

A total of 10 boreholes were drilled, reaching an aggregate depth of 210 m. The borehole depths range between 15 and 30 m, revealing alluvial soil deposits across the entire site (Figure 1). Based on visual and laboratory classifications, the subsoil mainly consists of CH (high-plasticity clay) and CL–CH (low- to high-plasticity transition clay) materials. The groundwater table was encountered between 5.0 and 10.0 m below the surface. These conditions emphasize the necessity of implementing dewatering and drainage control measures during the excavation phase.

Figure 1. Location map of the boreholes within the project site. (Proje sahası içerisindeki sondajların yer haritası)

Table 1 summarizes the elevation, coordinates, drilling depth, groundwater level, and lithological characteristics of the boreholes. The obtained data indicate that the subsurface strata are plastic, compressible, and moisture-sensitive alluvial soils with low drainage capacity, which can significantly influence the slope stability and foundation performance of the planned structure.

Table 1. Summary of borehole elevations, coordinates, depths, groundwater levels, and lithological units (Sondajlara ait kot, koordinat, derinlik, yeraltı suyu seviyesi ve litolojik birimlerin özeti)

Borehole ID	Elevation (m)	Depth (m)	Groundwater Level (m)	Lithology	Formation
BH-1	934	20	5.5	CL-CH	Alluvium
BH-2	934	20	5.0	CH	
BH-3	933	15	10	CH	
BH-4	933	15	10	CH	
BH-5	933	15	9.5	CH	
BH-6	933	15	6.5	CH	
BH-7	934	25	8.0	CL-CH	
BH-8	933	30	7.0	CH	
BH-9	933	25	8.0	CH	
BH-10	933	30	7.5	CH	

3. MATERIALS AND METHOD (MATERYAL VE METOD)

The methodological framework of this study consists of subsurface investigation, laboratory characterization, determination of geotechnical design parameters, constitutive modeling, and numerical simulation using the finite element method. All soil and structural parameters employed in the analyses are summarized in Tables 2–5. Two complementary numerical analysis approaches were adopted in this study. In the first stage, the limit equilibrium–based SLIDE program was utilized to evaluate the overall slope stability and to determine potential failure mechanisms under short-term (undrained) and long-term (drained) conditions. These analyses provided critical slip surfaces and safety factors for different excavation depths.

The fundamental index properties obtained from borehole sampling and laboratory classification tests are presented in Table 2, including natural water content (w_n), Atterberg limits (LL, PL, PI), USCS classification, natural unit weight (γn), and groundwater level (GWL). These baseline properties provide the foundation for assessing the engineering behavior of the soils and defining the geotechnical layers for numerical modeling

Table 2. Soil property parameters employed in the numerical analyses (Sayısal analizlerde kullanılan zemin özellik parametreleri)

	Layer-1	Layer-2	Layer-3	Layer-4
W_n (%)	33.2	32.6	23.4	20.5
LL (%)	63.1	61.7	56.4	58.8
PL (%)	29.2	27.7	27.1	27.9
PI (%)	34.0	34.9	29.3	30.8
USCS	CH	CL-CH	CH	CH
Υ_n (kN/m^3)	19.0	19.6	19.8	19.8
GWL	7.5 m			

Based on the soil classification results, shear strength parameters were determined from consolidated undrained triaxial and direct shear tests. The undrained shear strength (cu), effective cohesion (c′), and effective friction angle (φ′) used in the analyses are given in Table 3.

Table 3. Shear strength parameters adopted in the analyses (Analizlerde kullanılan kayma dayanımı parametreleri)

	Layer-1	Layer-2	Layer-3	Layer-4
c_u (kPa)	35	50	135	200
c’ (kPa)	3.5	5	13.5	20
Φ’ (˚)	25	25	26	26

The deformation characteristics governing soil stiffness behavior were determined through laboratory testing and empirical correlations. Undrained shear strength (cu), Poisson’s ratio (ν), undrained modulus (Eu), and secant modulus (Es) are summarized in Table 4. As noted by Poulos and Small (2000), the undrained deformation modulus can be converted to the drained shear modulus by multiplying it by 0.4 for soft clays and 0.6 for stiff clays, reflecting the stiffness contrast associated with drainage conditions [17]. This approach was adopted in the present study to derive drained stiffness parameters used in the finite element soil model.

Table 4. Undrained deformation modulus and Poisson's ratio (Drenajsız deformasyon modülü ve Poisson oranı)

	Layer-1	Layer-2	Layer-3	Layer-4
c_u (kPa)	35	50	135	200
υ	0.4	0.4	0.4	0.4
E_u	16000	22000	54000	80000
E_s	6400	13200	32400	48000

Following the determination of elastic and plastic soil parameters, the Hardening Soil (HS) model was adopted for the numerical analyses. The HS model is particularly suitable for field applications involving complex stress paths, such as deep excavations, where the yield surface evolves with the stress state. Compared with linear elastic–perfectly plastic models, the HS formulation provides a more realistic representation of soil stress–strain behavior under varying loading conditions, including nonlinear stiffness, plastic strain accumulation, and stress-dependent deformation.

In addition to the soil parameters, the structural reinforcement elements employed at the construction site were incorporated into the numerical model. The anchors were constructed with a bond length of 10 m, a root diameter of 0.15 m, and were prestressed to 32 tons. Based on these field installation properties, the axial load-carrying capacity of the anchors was calculated and used as boundary conditions within the finite element environment. The structural details including diameter (d), cross-sectional area (A), elastic modulus (E), Poisson's ratio (ν), moment of inertia (I), axial stiffness (EA), and flexural rigidity (EI) are provided in Table 5.

Table 5. Technical details of the structural elements

(Yapısal elemanlara ait teknik detaylar)

	Pile-1 (S_H=1.2m)	Pile-2 (S_H=1.5m)	Anchor Free Length (3*0.6'')	Anchor Bond Length (S_H=1.5m)
d (m)	0.65	1.0	-	0.15
A (m^2)	0.3318	0.79	0.00042	0.017
E (kPa)	30000000	30000000	$2x10^8$	21000000
υ	0.15	0.15	-	-
I (m^4)	0.0088	0.05	-	-
EA (kN/m)	8295000	15800000	-	238000
EA (kN)	-	-	84000	-
EI	9954000	23700000	-	-

All soil parameters and structural inputs were integrated into the finite element model to simulate slope behavior under static, pseudo-static, and seepage-affected conditions. Groundwater flow analysis was coupled with stability evaluation to

capture the development of pore-water pressures and their effect on potential slip surfaces.

4. RESULTS (SONUÇLAR)

The limit equilibrium analyses were first conducted in SLIDE to establish the baseline stability conditions and to identify the potential failure mechanism [18]. The site geometry was defined using a large model domain extending 150 m horizontally and 45 m vertically to eliminate boundary effects and ensure realistic stress distribution within the slope mass. Short-term undrained behaviour was evaluated through a $\varphi = 0$ analysis, which assumes undrained shear conditions consistent with saturated cohesive soils immediately after excavation. For long-term stability assessment, the Mohr–Coulomb shear strength parameters (cohesion c and friction angle φ) previously determined from laboratory tests were assigned to the corresponding soil layers. These analyses enabled the identification of the critical slip surface for both drainage conditions. Among the available limit equilibrium methods, the Spencer method was adopted due to its rigorous satisfaction of both force and moment equilibrium, providing a reliable factor of safety for the subsequent design stages.

As seen in Figure 2, the short-term undrained ($\varphi = 0$) analysis for the 5 m excavation produces a shallow critical slip surface with a low factor of safety. This represents the most critical condition immediately after excavation when excess pore pressures have not dissipated and shear resistance depends solely on undrained cohesion.

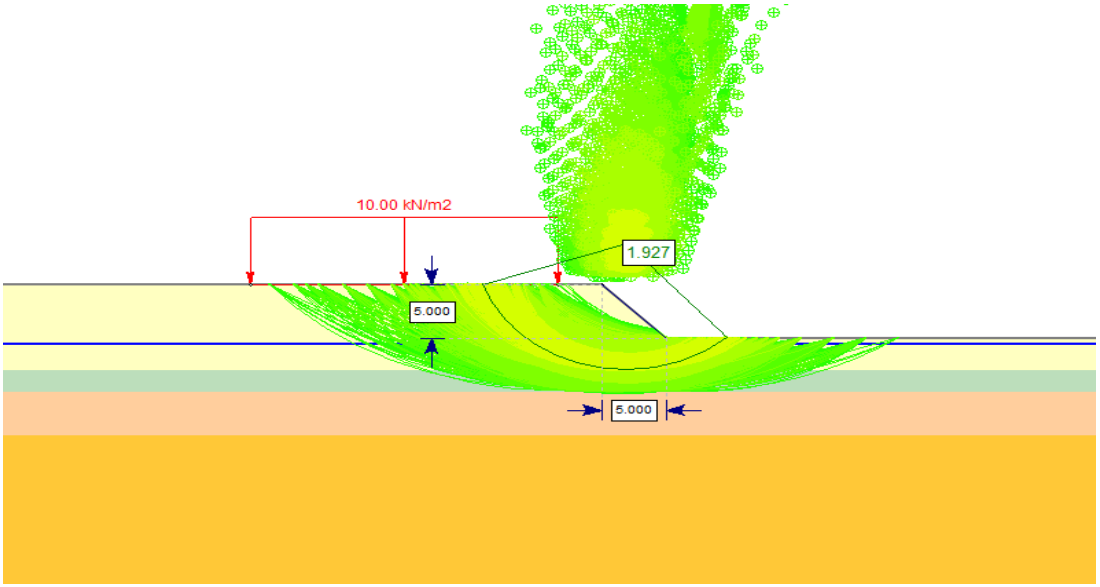

Figure 2. Short-term (undrained) stability analysis for the 5 m excavation. (5 m derinliğindeki kazı için kısa süreli (drenajsız) stabilite analizi)

Figure 3 demonstrates the long-term drained stability condition for the 5 m excavation. Dissipation of pore pressures allows mobilization of full Mohr–Coulomb parameters (c–φ), resulting in a deeper, more stable slip surface and increased factor of safety.

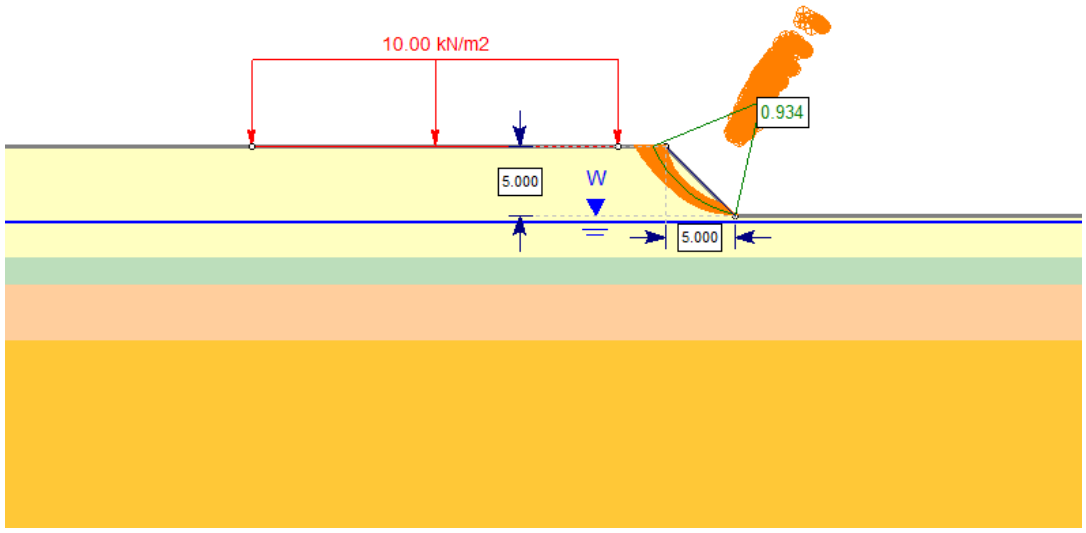

Figure 3. Long-term (drained) stability analysis for the 5 m excavation. (5 m derinliğindeki kazı için uzun süreli (drenajlı) stabilite analizi)

As indicated in Figure 4, increasing excavation depth to 6.5 m under short-term undrained conditions enlarges and deepens the failure mechanism due to increased lateral earth pressures and greater unsupported height.

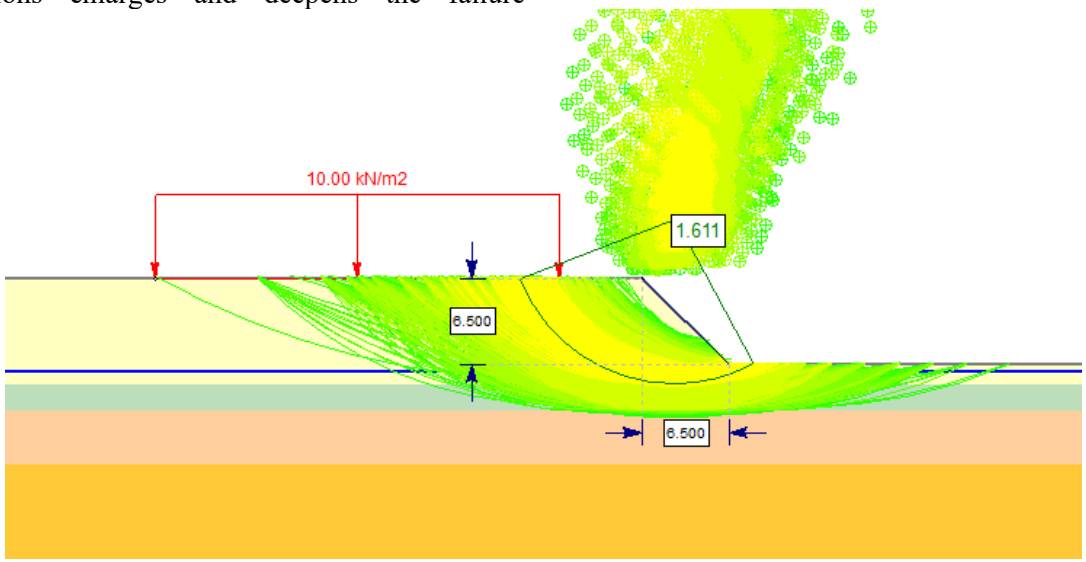

Figure 4. Short-term (undrained) stability analysis for the 6.5 m excavation. (6,5 m derinliğindeki kazı için kısa süreli (drenajsız) stabilite analizi)

Figure 5 shows that long-term drained behavior at 6.5 m excavation improves stability; however, the deeper slip surface still indicates potential for a global failure mechanism due to stress redistribution.

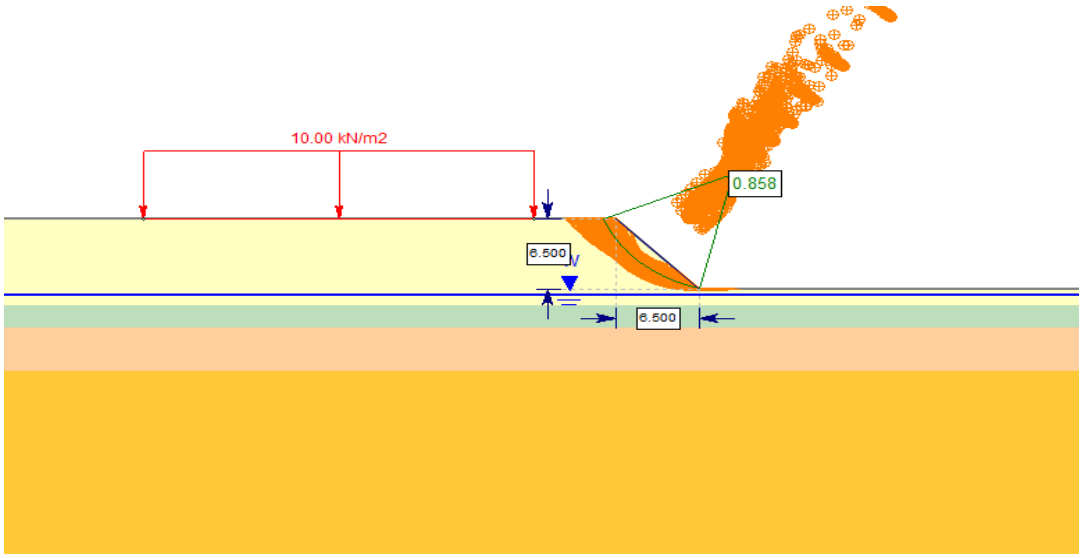

Figure 5. Long-term (drained) stability analysis for the 6.5 m excavation. (6,5 m derinliğindeki kazı için uzun süreli (drenajlı) stabilite analizi)

As summarized in Table 6, the limit equilibrium analyses indicate that while short-term undrained conditions yield safety factors exceeding the minimum acceptable threshold for both excavation depths, long-term drained conditions result in safety factors below 1.5, clearly highlighting the governing influence of groundwater dissipation and effective stress reduction on global slope stability.

Table 6. Factors of Safety Results from Slope Stability Analyses / (Şev stabilite analizlerinden elde edilen güvenlik katsayısı sonuçları)

		FS	*Min. FS*	
5.0 m excavation	Undrained	1.927	>1.5	P
	Drained	0.934	<1.5	X
6.5 m excavation	Undrained	1.611	>1.5	P
	Drained	0.858	<1.5	X

The SLIDE analyses were conducted to assess the global stability of the slope and to identify critical failure surfaces using limit equilibrium methods. Both undrained ($\varphi = 0$) and drained (c–φ) conditions were examined to establish baseline safety factors and failure mechanisms, which subsequently served as a reference framework for the finite element analyses.

Following the identification of the critical failure surface in SLIDE, detailed numerical analyses were performed in PLAXIS to design and evaluate the retaining system required for the critical portion of the slope. Two alternative systems—anchored retaining structures and piled retaining structures—were examined and compared in terms of force demand, deformation response, and achievable safety margin. As a preliminary step, the factor of safety (FS) values obtained from the limit-equilibrium analyses were evaluated for both drained and undrained conditions, indicating that FS exceeded the minimum acceptable level only in undrained analyses, whereas all drained scenarios yielded FS < 1.5 (Table 5).For the pile-supported option, the minimum embedment depth was determined by balancing shear forces and bending moments along the pile length, with the additional requirement that the pile toe must penetrate at least 3–4 m into the stiff claystone/rock layer to ensure adequate fixity and rotational restraint. Based on these considerations, the pile length was further increased to enhance structural stability and serviceability performance. These combined FS assessments and PLAXIS simulations provided a comprehensive understanding of soil–structure interaction and guided the selection of the most effective retaining system for the site.

In the Plaxis 2D analyses, two independent analysis sets were developed using the selected geotechnical

design parameters, and the corresponding results were comparatively evaluated [19]. This comparison focused on the applicability and cost-effectiveness of each support system. All analyses were performed using the Hardening Soil (HS) constitutive model, which provides a more realistic representation of soil behavior under complex loading conditions, particularly those analogous to deep-excavation environments within the framework of the relevant failure criteria.

The lateral static and pseudo-static displacement responses for the four retaining configurations are illustrated in Figure 6. Complementarily, the maximum shear force and bending moment distributions along the piles derived from PLAXIS finite element analyses are summarized for each design scenario to provide a comprehensive assessment of structural demand.

For the anchored system employing a 0.65-m diameter pile at a 5-m excavation depth, the maximum shear forces were determined as 42 kN/m under static loading and 540 kN/m under pseudo-static loading. The corresponding bending moments were calculated as 46 kNm/m and 1562 kNm/m, respectively, indicating a substantial increase in internal forces when seismic effects are considered.

In the second configuration, consisting of a 1.0-m diameter cantilever pile at the same excavation depth, the static and pseudo-static shear forces reached approximately 66 kN/m and 863.7 kN/m, respectively. The bending moments for this system were markedly higher than those of the anchored alternative, reaching 416 kNm/m under static loading and 1737 kNm/m under pseudo-static loading, reflecting the greater structural demand imposed on unsupported cantilever elements.

For the 6.5-m excavation depth supported by a 0.65-m diameter anchored pile, the maximum shear forces were obtained as 56 kN/m (static) and 52 kN/m (pseudo-static). The corresponding bending moments were 85 kNm/m and 95 kNm/m, indicating a relatively modest increase in internal forces under seismic loading for this configuration.

Accordingly, in pseudo-static earthquake analyses, the applied loading is not time-dependent; therefore, no new stress redistribution develops within the system. Instead, the existing static stress state is evaluated by superimposing a small horizontal seismic acceleration. As a result, settlements previously developed in the soil profile, pile or retaining wall displacements, and particularly the stiffness mobilized during the static phase—especially under the Hardening Soil constitutive model—are directly transferred into the pseudo-static seismic stage. Consequently, when a relatively small seismic coefficient is adopted or when the soil has already attained a high stiffness during the static loading phase, the internal forces obtained from the pseudo-static analysis may not exceed those computed under static conditions and, in some cases, may even be lower. Moreover, a change in the direction of the applied seismic load can modify the active–passive earth pressure equilibrium, potentially leading to a reduction in shear forces. For these reasons, the pseudo-static approach should be regarded as an approximate method that does not fully capture real earthquake behavior, as it neglects inertia effects and dynamic soil–structure interaction. Accordingly, as widely reported in the literature, it is both common and expected that shear forces obtained from static analyses may exceed those calculated in the pseudo-static seismic phase.

Finally, the 6.5-m deep excavation supported by a 1.0-m diameter cantilever pile exhibited significantly higher internal forces. The maximum shear forces reached 147 kN/m in the static analysis and 600 kN/m in the pseudo-static analysis, while the bending moments increased to 735 kNm/m (static) and 1900 kNm/m (pseudo-static). These results highlight the heightened bending and shear demands that occur when excavation depth increases in the absence of anchorage support.

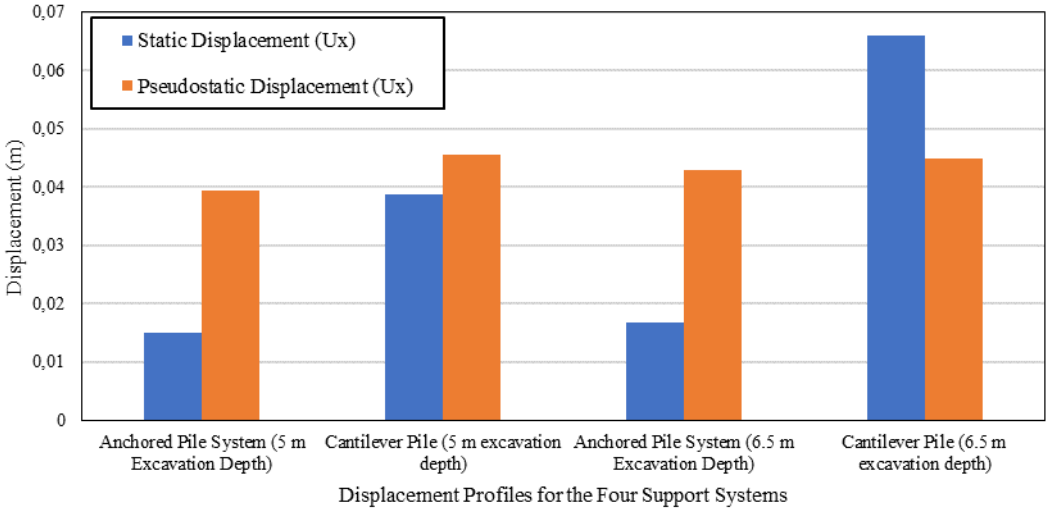

Figure 6. Horizontal Displacement Profiles for the Four Support Systems -Static and Pseudo-static Analyse. (Dört farklı destek sistemi için statik ve pseudo-statik analizlere ait yatay deplasman profilleri)

Across all configurations, PLAXIS output diagrams consistently show that the peak shear forces and bending moments concentrate near the pile toe. This behavior aligns with established theoretical expectations, reflecting the mobilization of passive resistance and the dominance of bending stiffness under increasing lateral soil pressures induced by excavation. The observed distribution underscores the necessity of adequate pile embedment to ensure rotational fixity and structural reliability under both static and seismic loading conditions.

5. CONCLUSIONS (SONUÇLAR)

This study presents a comprehensive geotechnical assessment of excavation induced slope instability for a construction site located in Bağlıca, Etimesgut (Ankara). Through the integration of field investigations, laboratory testing, limit equilibrium analyses, and advanced finite element modelling, the research provides an in-depth evaluation of the mechanisms governing slope behavior under static, pseudo-static, and seepage conditions. The analytical findings clearly demonstrate that groundwater regime, soil plasticity characteristics, and stress redistribution associated with excavation act as the principal factors controlling instability. Elevated pore-water pressures particularly within the CH and CL–CH layers significantly reduced the effective stress state, promoting shallow and circular slip surfaces. These findings are consistent with previous studies showing that even minor fluctuations in hydraulic conductivity and groundwater level can critically affect stability margins in clay-rich alluvial deposits.

A detailed comparison of retaining system performance was conducted for excavation depths of 5 m and 6.5 m using PLAXIS simulations. For the 5 m excavation, the anchored system consisting of 1.2 m diameter piles with horizontal and vertical anchor spacing of 1.2 m and 1.5 m, respectively produced a horizontal displacement of 1.5 cm, which satisfies the allowable deformation criterion of $\delta H = 0.003H$. The corresponding cantilever system, constructed with a 1.5 m diameter pile, yielded a horizontal displacement of 3.8 cm, remaining within the permissible limit of $\delta H = 0.01H$. At 6.5 m excavation depth, the anchored configuration again achieved satisfactory performance with a displacement of 1.6 cm, while the cantilever system reached 6.6 cm, still compliant with serviceability requirements. These comparative results reinforce that anchored systems offer superior lateral deformation control, demonstrating smaller displacements and improved structural efficiency relative to cantilever piles at both excavation depths.

Shear force and bending moment distributions revealed that structural demand concentrates primarily near the pile toe, underscoring the necessity of sufficient embedment into the stiff underlying layer to provide rotational fixity and adequate passive resistance. The Hardening Soil model effectively captured the nonlinear stiffness behavior and plastic strain accumulation associated with excavation processes, confirming its applicability to complex stratigraphies characterized by soft-to-stiff clay transitions and variable groundwater conditions.

Overall, the study emphasizes that reliable evaluation of deep excavations in moisture-sensitive clayey soils requires a multi-parameter, hydro-mechanically coupled analytical approach.

The incorporation of seepage effects, stress-dependent stiffness parameters, and realistic boundary conditions significantly enhances the accuracy of stability predictions. The anchored retaining system ultimately emerges as the most technically robust and serviceable solution for the examined site, providing effective displacement control, improved performance under dynamic and pseudo-static loads, and optimized structural response. The methodologies and findings presented herein contribute to the wider geotechnical literature by demonstrating the importance of combining high-quality field data with advanced constitutive modelling for assessing excavation-induced stability within heterogeneous geomaterials and fluctuating groundwater regimes, offering a practical reference framework for similar urban construction environments.

DECLARATION OF ETHICAL STANDARDS (ETİK STANDARTLARIN BEYANI)

The author of this article declares that the materials and methods they use in their work do not require ethical committee approval and/or legal-specific permission.

Bu makalenin yazarı çalışmalarında kullandıkları materyal ve yöntemlerin etik kurul izni ve/veya yasal-özel bir izin gerektirmediğini beyan ederler.

AUTHORS' CONTRIBUTIONS (YAZARLARIN KATKILARI)

The authors have contributed equally to the work.

Yazarlar çalışmaya eşit oranda katkı sağlamıştır.

CONFLICT OF INTEREST (ÇIKAR ÇATIŞMASI)

There is no conflict of interest in this study.

Bu çalışmada herhangi bir çıkar çatışması yoktur.

REFERENCES

[1] Erdağ, A. (2021). Slope Stability Evaluation of Basement Excavation: A Case Study. Düzce Üniversitesi Bilim ve Teknoloji Dergisi, 9(5), 1936-1948.

[2] Li, L., Wang, Y., Zhang, L., Choi, C., & Ng, C. W. (2019). Evaluation of critical slip surface in limit equilibrium analysis of slope stability by smoothed particle hydrodynamics. International Journal of Geomechanics, 19(5), 04019032.

[3] Pınarlık, M., Kardoğan, P. S. Ö., & Demircan, R. K. (2017). Şev stabilitesine zemin özelliklerinin etkisinin limit denge yöntemi ile irdelenmesi. Mühendislik Bilimleri ve Tasarım Dergisi, 5(3), 675-684.

[4] Khan, M. I., Fei, J., Chen, X., & Chen, Y. (2025). Usage of permeability ratio to check the stability of a pile-soil model with retaining wall support–Huizhou slope failure as a case study. *International Journal of Geo-Engineering*, *16*(1), 7.

[5] Park, S., Kim, W., Lee, J., & Baek, Y. (2018). Case study on slope stability changes caused by earthquakes—focusing on Gyeongju 5.8 ML EQ. Sustainability, 10(10), 3441.

[6] Erdağ, A., & Kardoğan, P. S. Ö. (2022). Experimental study on plastic waste application for soil stabilization. Environmental Engineering & Management Journal (EEMJ), 21(9).

[7] He, Y., Li, B., & Du, X. (2023). *Soil Slope Instability Mechanism and Treatment Measures under Rainfall—A Case Study of a Slope in Yunda Road. Sustainability, 15 (2), 1287*.

[8] Çavuşoğlu, İ., & Alemdağ, S. (2025). Taş Ocağında Patlatmalı Kazı Kaynaklı Zemin Titreşimleri, Hava Şoku ve Şev Duraylılığının İncelenmesi: Örnek Bir Uygulama. Doğal Afetler ve Çevre Dergisi, 11(2), 557-571.

[9] Karaca, G. B. G., Ordu, Ş., & Ordu, E. (2025). Katı Atık Depolama Sahalarındaki Stabilite Sorunlarının Araştırılması. Doğal Afetler ve Çevre Dergisi, 11(1), 70-88.

[10] Ün, B., & Yıldız, A. (2021). Şev stabilitesi probleminin geri analizle çözümü: örnek bir vaka. Academic Platform-Journal of Engineering and Science, 9(1), 174-181.

[11] Erdağ, A., & Kardoğan, P. S. Ö. (2022). Experimental study on plastic waste application for soil stabilization. Environmental Engineering & Management Journal (EEMJ), 21(9).

[12] Kardoğan, P. Ö., & Erdağ, A. (2022). The Effects of Construction Waste on Climate Change: Is a More Green Construction Industry Possible?. Mühendislik Bilimleri ve Tasarım Dergisi, 10(4), 1222-1231.

[13] Erdağ, A., Çetin, B., & Fırat, S. (2025). Evaluation of resilient modulus and permanent deformation of steel slags and subgrade soil stabilized with geogrid material. Construction and Building Materials, 471, 140640.

[14] Erdağ, A., Fırat, S., Fares, M. Y., Işık, N. S., & Cetin, B. (2025). Performance evaluation of geogrid-stabilized steel slag layer of pavement under repeated cyclic loading. Transportation Geotechnics, 101603.

[15] Oztekin, B., Topal, T. A. M. E. R., & Kolat, C. (2006). Assessment of degradation and stability of a cut slope in limestone, Ankara-Turkey. Engineering Geology, 84(1-2), 12-30.
[16] AFAD (2018). Afet ve Acil Durum Yönetimi Başkanlığı. https://www.afad.gov.tr/ (Erişimtarihi: 5.10.2018)
[17] Poulos, H. G., & Small, J. C. (2000). ground slabs. Design Applications of Raft Foundations, 39.
[18] Rocscience Inc., Slide 2D Manual, Version 6.020, 2012.
[19] Bentley Advancing Infrastructure ‹Manual Models Material for Plaxis 2D ‹Connect Edition V22.00 ,2021.